Biosensors and Bioelectronics 80 (2016) 201–207

Contents lists available at ScienceDirect

Biosensors and Bioelectronics

journal homepage: www.elsevier.com/locate/bios

Simultaneous immunoassay of phosphorylated proteins based on apoferritin templated metallic phosphates as voltammetrically distinguishable signal reporters

Xiaoxiao Ge [a,b], Aidong Zhang [a], Yuehe Lin [a,b,c], Dan Du [a,b,c,*]

[a] Key Laboratory of Pesticide and Chemical Biology of Ministry of Education, College of Chemistry, Central China Normal University, Wuhan 430079, PR China
[b] School of Mechanical and Materials Engineering, Washington State University, Pullman, WA 99164, United States
[c] Paul G. Allen School for Global Animal Health, Washington State University, Pullman, WA 99164, United States

ARTICLE INFO

Article history:
Received 17 November 2015
Received in revised form
21 January 2016
Accepted 23 January 2016
Available online 24 January 2016

Keywords:
Simultaneous immunoassay
Apoferritin templated metallic phosphates
Phoaphorylated protein
Electrochemical detection

ABSTRACT

A novel electrochemical immunosensor has been developed to detect phosphorylated proteins, phospho-p53^{15} and phospho-p53^{392}, simultaneously. Different apoferritin templated metal phosphates were used as distinguishable signal reporters (apoferritin templated cadmium phosphates (ATCP) and apoferritin templated lead phosphates (ATLP)) to enhance the detection sensitivity. Here, magnetic Fe_3O_4 nanoparticles functionalized phospho-p53^{15} capture antibody (MP-p53^{15} *c*-Ab) and phospho-p53^{392} capture antibody (MP-p53^{392} *c*-Ab), respectively, were used to specifically capture phospho-p53^{15} and phospho-p53^{392} antigens, followed by immunorecognition with p53^{15} detection antibody (p53^{15} *d*-Ab) and p53^{392} detection antibody (p53^{392} *d*-Ab) to form sandwich-like immunocomplexes. SiO_2@Au nanocomposites served as nanocarriers for co-immobilization of both d-Ab and signal reporters (ATCP/SiO_2@Au/p53^{15} *d*-Ab, ATLP/SiO_2@Au/p53^{392} *d*-Ab), which greatly amplified the detection signal. The distinguished current responses were achieved by electrochemical detection of cadmium ions and lead ions with square wave voltammetry (SWV) after dissolution with acid. The proposed immunoassay exhibited high sensitivity and selectivity for the detection of phospho-p53^{15} and phospho-p53^{392} simultaneously. The linear relationships between electrochemical responses and the concentrations of phospho-p53^{15} and phospho-p53^{392} were obtained in the range of 0.1–20 ng/mL and 0.05–20 ng/mL, respectively. The detection limits were 0.05 and 0.02 ng/mL ($S/N=3$), respectively. This strategy provides a new platform for simultaneous immunoassay of multiple protein biomarkers.

1. Introduction

Protein phosphorylation is a major regulatory mechanism, which controls many basic cellular processes and affects part of the proteome (Ptacek et al., 2005). p53 protein, a well-known tumor suppressor, usually plays a critical role in regulating cell growth and DNA repair processes. It is also a potent transcription factor in cellular responses to various stress signals, such as ionizing radiation and UV induction (Vousden and Lane, 2007; Evan and Vousden, 2001; Appella and Anderson, 2001; Toledo and Wahl, 2006). Once stimulated, the p53 protein native conformation would be affected and the phosphorylation of p53 on several amino acid residues would be increased, which may directly result in genomic instability and tumor development (Bode and Dong, 2004; Bernal et al., 2007; Ashcroft et al., 1999; Minamoto et al., 2001). It has been reported that phosphorylation at serine 392 in human p53 may be involved in human breast tumor and ovarian neoplasms (Bar et al., 2009; Yap et al., 2004); and serine 15 in human p53 is specially phosphorylated by ionizing radiation and UV, which may damage the DNA repair process (Kazuyasu et al., 2013). Thus, these specific phosphorylation sites of p53 are useful biomarkers of diseases. Simultaneous detection of multiple phosphorylated p53 at different sites is significant for early diagnosis and treatment of tumor diseases.

Compared with parallel detection of a single biomarker, simultaneous detection of multiple biomarkers improved detection efficiency, including shortened analytical time, decreased sample volume and reduced cost. Simultaneous immunoassay of multiplex analytes has been reported in recent publications (Wilson and Nie, 2006; Tang et al., 2011; Du et al., 2011a,b,c). For example, Wilson and Nie (2006) reported an array-based electrochemical sensor for immunoassay of four different analytes on an SPE at the same time. Tang et al. (2011), developed a multiple immunosensor

* Corresponding author at: Key Laboratory of Pesticide and Chemical Biology of Ministry of Education, College of Chemistry, Central China Normal University, Wuhan 430079, PR China.
E-mail address: dan.du@mail.ccnu.edu.cn (D. Du).

http://dx.doi.org/10.1016/j.bios.2016.01.058
0956-5663/

based on distinguishable signal tags for simultaneous detection of carcinoembryonic antigen and alpha-fetoprotein. Our group developed a multiplexed electrochemical immunosensor array based on electric field-driven acceleration for assay of phosphorylated p53 in different phosphorylation sites, in which enzyme-functionalized gold nanorod was carried as signal reporter and signal amplification (Du et al., 2011b). Simultaneous electrochemical immunoassay of multiple analytes has attracted more and more attention due to its superiority. Among all the reported methods, immunoassay of multiple analytes was designed either by sensor array or by using distinguishable signal reporters.

Recently, nanomaterials have been used to amplify the detection signal in biosensors (Zhu et al., 2015a,b; Ge et al., 2014; Zhang et al., 2014). These nanomaterials included gold nanoparticles (Lai et al., 2011, Jiang et al., 2016), quantum dots (Wang et al., 2008a,b; Lin et al., 2008), carbon nanotubes (Yu et al., 2006), carbon nanospheres (Du et al., 2010), graphene oxide (Du et al., 2011b; Song et al., 2016; Yang et al., 2013), and silica nanoparticles (Wu et al., 2009; Yuan et al., 2011; Tang et al., 2008). Protein cages have been reported as an immuno-labels to enhance detection sensitivity (Zhao et al., 2015). Apoferritin is the most commonly used protein case. It is constituted with 24 polypeptide subunits that self-assemble into a hollow cage with an interior diameter of 8 nm and an exterior diameter of 12 nm (Uchida et al., 2007; Shin et al., 2010). There are 14 channels formed at subunit intersections, including 6 hydrophobic channels and 8 hydrophilic channels, and the channels are ~3–4 nm in diameter (Okuda et al., 2003; Iwahori et al., 2005; Liu et al., 2007, 2006). Therefore, apoferritin can act as a nanoreactor to synthesize metal nanocomposites inside, such as iron phosphate (Polanams et al., 2005), cadmium sulfide (Wong and Mann, 1996), and other nanomaterials (Douglas et al., 1995), for signal amplification of immunosensors. We have successfully synthesized lead phosphates in the interior of apoferritin by diffusion as signal reporters in immunoassay (Du et al., 2011b; Chen et al., 2012). Most importantly, the interior of apoferritin can be used to synthesize different metal phosphates in the same reaction condition to act as distinguishable signal reporters for simultaneous immunoassay of multiple analytes.

Herein, we reported a new technique for simultaneous immunoassay of two analytes: phospho-p53^{15} and phospho-p53^{392} by synthesizing voltammetrically distinguishable metal phosphates in the cavity of apoferritin (apoferritin templated cadmium phosphate (ATCP) and apoferritin templated lead phosphate (ATLP)) as signal reporters. The amplification was further achieved by using SiO_2/Au nanocomposites as nanocarriers to immobilize more signal reporters. The captured signal reporters (ATCP, ATLP) were detected by square wave voltammetry (SWV) after release from apoferritin.

2. Experiment methods

2.1. Reagents and materials

Human phospho-p53^{15} ELISA kit, which included phospho-p53^{15} capture antibody, phospho-p53^{15} antigen, and biotin-phospho-p5315 detection antibody, and Human phospho-p53^{392} ELISA kit were purchased from R&D Systems Inc. Carboxyl-functionalized monodispersed magnetic particles (MPs, 5 mg/mL) were purchased from Baseline Chromtech (Tianjin, China). Apoferritin, bovine serum albumin (BSA), 1-ethyl-3-(3-dimethylaminopropyl) carbodiimide hydrochloride (EDC), N-hydroxysuccinimide (NHS), 2-(N-morpholino)ethanesulfonic acid (MES), and Tween-20 were purchased from Sigma-Aldrich. Tetraethox-ysi lane (TEOS, 98%) was purchased from Merck (Darmstadt, Germany). N-hydroxysuccinimide-acticated hexa-(ethylene glycol) undecane thiol (HS~NHS) was obtained from Nano Science Instrument Inc. (Phoenix, AZ). Chloroauric acid ($AuCl_3 \cdot HCl \cdot 4H_2O$, 96%) and trisodium citrate (99%) were obtained from Shanghai Chemical Reagent Co. (Shanghai, China). Lead nitrate, cadmium chloride, ethanol (EtOH, 98%), ammonium hydroxide ($NH_3 \cdot H_2O$, 25–28%), phosphate buffered saline (PBS) and Tris–HCl were acquired from Shenshi Reagent Co. (Wuhan, China). All solutions were prepared with distilled water.

2.2. Instruments

Electrochemical experiments, including cyclic voltammetry (CV) and square wave voltammetry (SWV) were performed on CHI 660C electrochemical analyzer (Shanghai China). A disposable screen-printed electrode (SPE), consisting of a carbon working electrode, a carbon counter electrode and an Ag/AgCl reference electrode, was purchased from Dropsens Inc. (Spain). The SPE was connected to the CHI electrochemical analyzer via a sensor connector (Dropsens Inc.). The electrochemical quartz crystal microbalance measurement (EQCM) was from Ivium Technologies (Netherlands) and was composed of a QCM200 quartz crystal microbalance. Field-emission scanning electron microscopy (FE-SEM) was performed using JEOL-6700F (JEOL, Tokyo, Japan). UV–vis spectra were obtained with a UV-2250 spectrophotometer (Japan).

2.3. Preparation of magnetic Fe_3O_4 nanoparticle functionalized antibodies

Magnetic Fe_3O_4 nanoparticle functionalized antibodies (MP-p53^{15} *c*-Ab, MP-p53^{392} *c*-Ab) were prepared by co-incubating p53^{15} captured antibody (p53^{15} *c*-Ab) and p53^{392} captured antibody (p53^{392} *c*-Ab) with activated magnetic Fe_3O_4 nanoparticles, respectively. Briefly, 10 μL, 5 mg/mL of carboxyl-functionalized MPs was activated with 100 mM EDC and 100 mM NHS solution in pH 5.2 MES buffer for 30 min. After magnetic separation and washing with buffer, the obtained activated MPs were dispersed in 1.0 mL pH 7.4 PBS for 10 min sonication, forming a monodispersed solution. Then 20 μL, 300 μg/mL of p53^{15} Ab_1 was added into the activated MPs solution and incubated for 2 h at room temperature. Subsequently, the mixture was magnetically separated and washed three times with PBS (pH 7.4) buffer containing 0.05% Tween-20 to remove excess antibodies. The resultant MP-p53^{15} *c*-Ab conjugates were re-dispersed in 1.0 mL PBS (pH 7.4) with 0.1% BSA and stored at 4 °C. The MP-p53^{392} *c*-Ab was prepared and stored using the same procedure.

2.4. Synthesis of ATCP/SiO_2@Au/p53^{15} d-Ab and ATLP/SiO_2@Au/p53^{392} d-Ab

2.4.1. Synthesis of ATCP and ATLP

ATCP nanoparticles and ATLP nanoparticles were synthesized according to our previous method (Du et al., 2011b; Liu and Lin, 2007). As illustrated in Scheme 1A, 500 μL 1 mg/mL lead nitrate solution ($Pb(NO_3)_2$) was introduced drop by drop to 2.0 mL 1 mg/mL apoferritin pre-diluted with pH 8.0 Tris–HCl buffer under stirring and the reaction proceeded for 1 h to allow the lead ions to diffuse into the cavity of apoferritin. 250 μL PBS (pH 7.0) was then added slowly to the above solution for forming metal phosphate core inside apoferritin protein cage. Excessive lead ions outside apoferritin were precipitated with PBS (pH 7.0) buffer. Afterward, the resulting solution was purified by directly dialysing with Tris–HCl (pH 8.0) for 72 h to obtain ATLP. ATCP nanoparticles were synthesized with cadmium chloride ($CdCl_2$) in light of the above procedure.

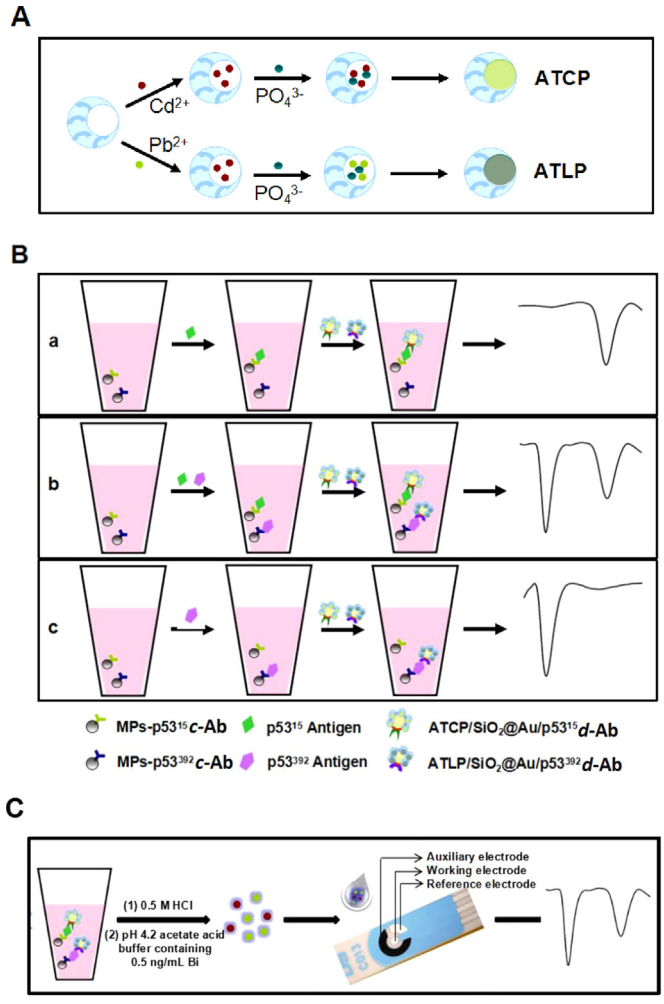

Scheme 1. (A) Synthesis illustration of Apoferritin templated metallic phosphates; (B) schematic illustration of simultaneous-immune-detection of multiple phosphorylated proteins: sandwich-like immunereaction with phospho-p53[15] (a), phospho-p53[15] and phospho-p53[392] (b), phospho-p53[392] (c). (C) The electrochemical measurement of multiple analyts.

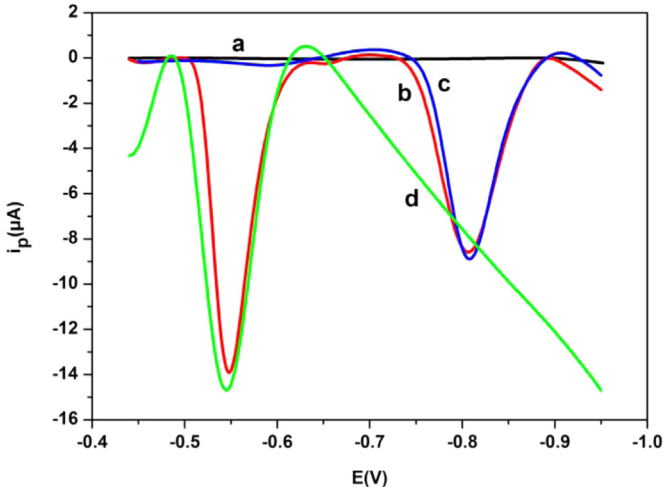

Fig. 1. SWV response of the simultaneous immune-detection sensor for MPs-p53[15] *c*-Ab and MPs-p53[392] *c*-Ab (a), 20 ng/mL phospho-p53[15] and 20 ng/mL phospho-p53[392] (b), 0 ng/mL phospho-p53[392] and 20 ng/mL phospho-p53[15] (c) and 20 ng/mL phospho-p53[392] and 0 ng/mL phospho-p53[15] (d).

2.4.2. Synthesis of SiO_2@Au NPs

The SiO_2@Au nanoparticles were synthesized in accordance with the procedure reported by Yang et al. (2012). First, the solutions of TEOS, EtOH, $NH_3 \cdot H_2O$ and H_2O (1:15:3:3, v/v) were filled simultaneously into the round-bottomed flask, followed by stirring for 4 h to obtain a white turbid suspension. Then the residue was separated and washed by centrifugation with ethanol and ultrapure water, and the obtained SiO_2 nanospheres were dried under vacuum for future use. Second, 100 mg SiO_2 nanospheres prepared above were dispersed in 50 mL 0.01% $HAuCl_4$ solution and sonicated for 1 min. Under vigorous stirring, the obtained mixed solution was heated to boiling, followed by quickly adding 800 μL 1.0% trisodium citrate and was kept boiling until the solution became pink. Ultimately, by centrifugation with ultrapure water, the product SiO_2@Au nanocomposites were obtained and re-dispersed in 50 mL pH 7.4 PBS buffer solution for future use.

2.4.3. Synthesis of ATCP/SiO_2@Au/p53[15] *d*-Ab and ATLP/SiO_2@Au/p53[392] *d*-Ab conjugates

To prepare ATCP/SiO_2@Au/p53[15] *d*-Ab conjugates, 5 mL SiO_2@Au nanocomposites were first activated with 20 μL 10 mM HS∼NHS under stirring for 30 min to form SiO_2@Au-NHS. After centrifugation with ultrapure water and re-dispersion in 5 mL PBS buffer (pH 7.4), 30 μL 2.0 mg/mL ATCP and 40 μL 7.0 μg/mL p53[15] *d*-Ab were added simultaneously and kept stirring overnight. The unbound ATCP and p53[15] *d*-Ab were removed by centrifugation and washing with PBS buffer. The obtained ATCP/SiO_2@Au/p53[15] *d*-Ab conjugates were re-dispersed in 2.0 mL pH 7.4 PBS containing 1% BSA and stored at 4 °C for use. ATLP/SiO_2@Au/p53[392] *d*-Ab conjugates were prepared using the same procedure.

2.5. Electrochemical immunoassay of phospho-p53[15] and phospho-p53[392]

Simultaneous detection of phospho-p53[15] and phospho-p53[392] was performed using two steps: immunorecognition (Scheme 1B) and ion-detection on the SPE (Scheme 1C). For traditional immunoassay, 25 μL MP-p53[15] *c*-Ab conjugates and 25 μL MP-p53[392] *c*-Ab conjugates pre-introduced into one centrifuge tube were incubated first with 25 μL phospho-p53[15] solution and 25 μL phospho-p53[392] solution for 60 min. After separation and washing, 50 μL of ATCP/SiO_2@Au/p53[15] *d*-Ab conjugates and 50 μL ATLP/SiO_2@Au/p53[392] *d*-Ab conjugates were added into the tube to complete immunoreactions. Discarding the unattached signal reporter conjugates by magnetic separation, the resulting immunecomplexes MP-p53[15] *c*-Ab-phospho-p53[15]-p53[15] *d*-Ab/SiO_2@Au/ATCP and MP-p53[392] *c*-Ab-phospho-p53[392]-p53[392] d-Ab/SiO_2@Au/ATLP were mixed with 30 μL HCl (0.5 M) for 5 min to release the cadmium and lead ions from ATCP and ATLP. After incorporation with 50 μL pH 4.2 acetate acid buffer containing 0.5 mg/mL Bi, the obtained ion solution of 50 μL was dropped onto the SPE to carry out electrochemical detection. The metal ions were first accumulated at −1.2 V for 2 min and followed by a SWV measurement by scanning from −1.0 V to −0.3 V with a step potential of 4 mV, amplitude of 25 mV and frequency of 15 Hz (Scheme 1C).

3. Results and discussion

3.1. Electrochemical behavior of the immunosensor

Simultaneous immuno-detection of phospho-p53[15] and phospho-p53[392] was performed based on SiO_2@Au nanocomposites as carriers and different apoferritin templated metallic phosphates as distinguishable signal reporters to enhance assay sensitivity. The electrochemical response was shown in Fig. 1. The MP-p53[15] *c*-Ab

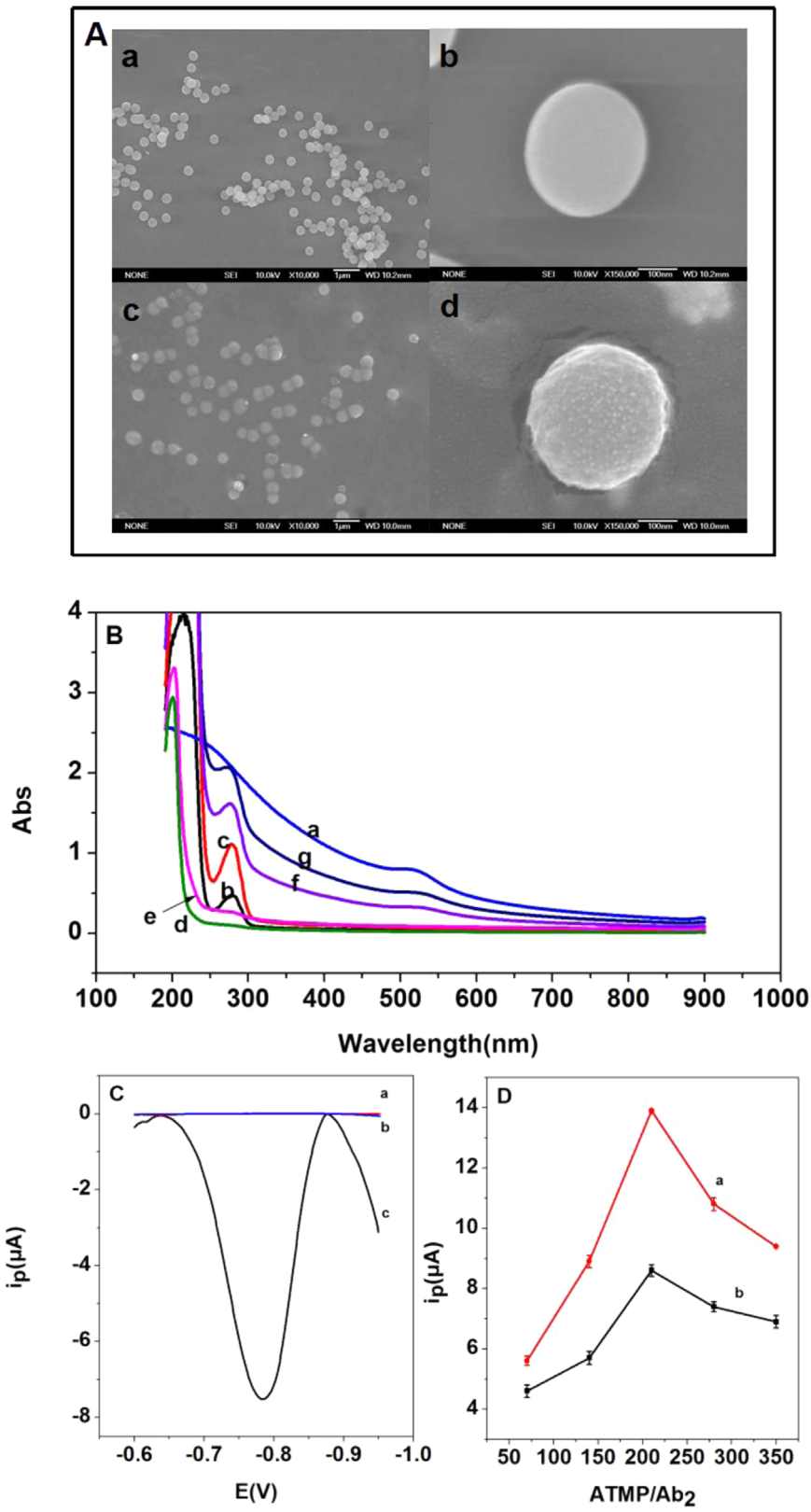

Fig. 2. (A) SEM images of SiO_2 (a and b) and SiO_2@Au (c and d) nanoparticles. (B) UV–vis spectra of SiO_2@Au (a), $p53^{15}$ *d*-Ab (b), $p53^{392}$ *d*-Ab (c), ATCP (d), ATLP (e), ATCP/SiO_2@Au/$p53^{15}$ d-Ab (f) and ATLP/SiO_2@Au/$p53^{392}$ *d*-Ab (g). (C) SWV response of the solution containing different analytes: SiO_2@Au (a), $p53^{15}$ *d*-Ab (b), ATCP/SiO_2@Au/$p53^{15}$ *d*-Ab (c). (D) the rate of signal reporters (ATMP) and Ab: ATLP and $p53^{392}$ *d*-Ab (a), ATCP and $p53^{15}$*d*-Ab (b).

and MP-$p53^{392}$ *c*-Ab solution did not show any detective signal (curve a), while after sandwich immunoreaction, two apparent current signals were observed at −0.808 V and −0.547 V (curve b), respectively, which resulted from the Cd^{2+} and Pb^{2+} ions by acid dissolution of the introduced ATCP and ATLP. However, there are very low signals even if no target antigen or only BSA was presented in the solution due to nonspecific absorption. And as expected, there was an obvious signal at −0.808 V if only

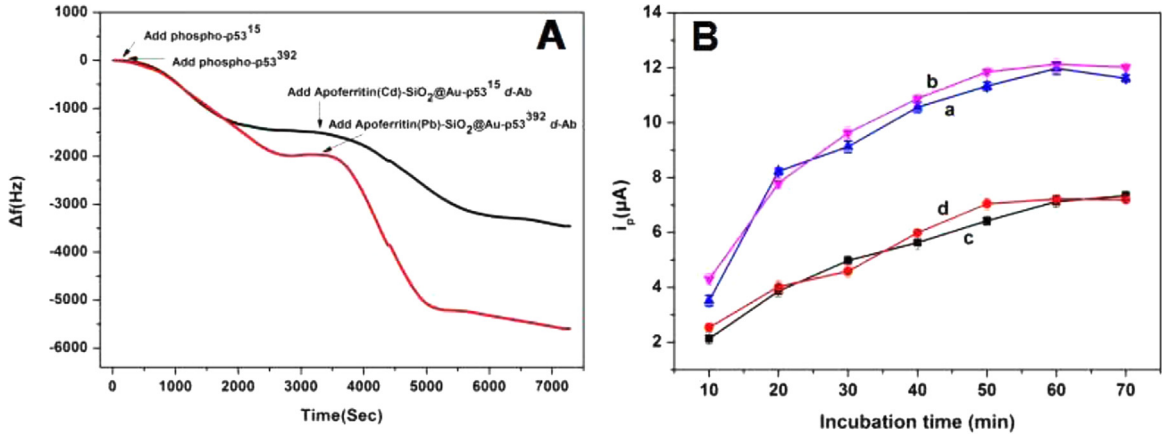

Fig. 3. (A) QCM response of the immune-affinity between antigen and antibodies. (B) Optimization of incubation time between nanomaterial-functionalized antibody and antigen: p53^{392} *c*-Ab and phospho-p53^{392} (a), phospho-p53^{392} and p53^{392} *d*-Ab (b), p53^{15} *c*-Ab and phospho-p53^{15} (c), phospho-p53^{15} and p53^{15} *d*-Ab (d).

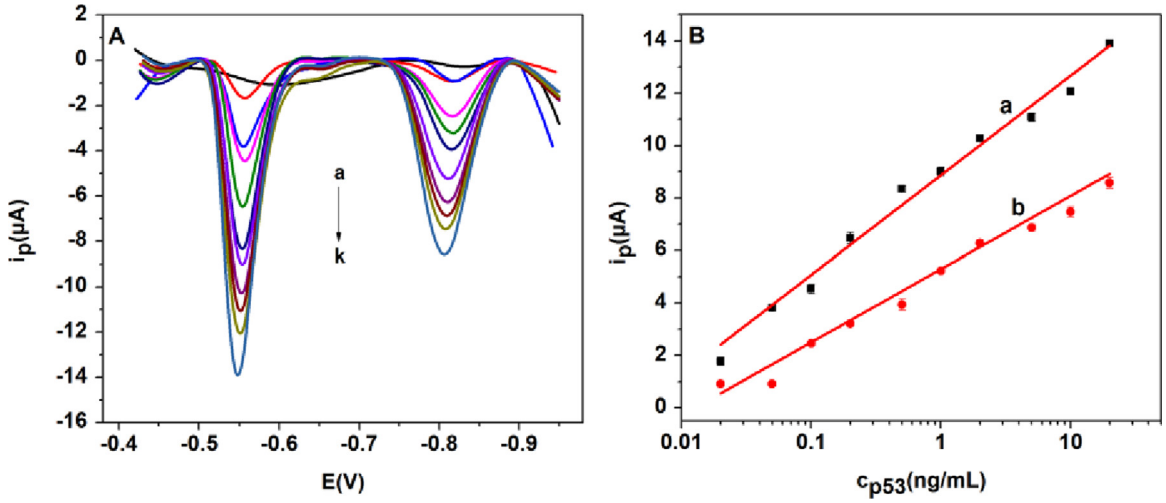

Fig. 4. (A) SWV response of the proposed simultaneous immunoassay with different concentration of phospho-p53^{392} (left) and phospho-p53^{392} (right): 0 ng/mL, 0.02 ng/mL, 0.05 ng/mL, 0.1 ng/mL, 0.2 ng/mL, 0.5 ng/mL, 1.0 ng/mL, 2.0ng/mL, 5.0 ng/mL, 10.0 ng/mL, 20.0 ng/mL. (B) Calibration curve of different concentration target analytes: phospho-p53^{392} (a) and phospho-p53^{15} (b).

Table 1
The assessment of the reliability of proposed dual-immune-detection sensor.

Sample no.	1		2		3	
Sample species	p53^{15}	p53^{392}	p53^{15}	p53^{392}	p53^{15}	p53^{392}
Add (ng/mL)	0.1	0	1.0	2.0	5.0	5.0
Found (ng/mL)	0.102	0.005	0.935	2.131	4.962	4.847
Recovery (%)	102	–	93.5	106.6	99.2	96.9

phospho-p53^{15} existed in the solution (curve c) and the obvious peak at −0.547 V was observed in phospho-p53^{392} solution (curve d). The strong immunoaffinity among MP *c*-Ab, phospho proteins and *d*-Ab conjugates showed no cross-talk during the multiplex immunoassay.

3.2. Characterization of ATCP/SiO$_2$@Au/p53^{15} d-Ab and ATLP/SiO$_2$@Au/p53^{392} d-Ab conjugates

SEM (Fig. 2A) shows smooth spherical structure of the synthesized SiO_2 nanoparticles with an average diameter of 200 nm (a and b). After modification with Au nanoparticles, the obtained SiO_2@Au nanocomposites exhibited relatively rough surfaces. The Au nanoparticles loaded on the surface of SiO_2 displayed an average diameter of 12 nm (c and d). Compared with pure SiO_2 nanoparticles, the introduction of Au nanoparticles not only increased surface area, but also made nanocomposites easier to be bio-functionalized with co-immobilization of both signal reporters and antibody.

UV–vis spectroscopy and SWV were further used to characterize the bio-conjugates of ATCP/SiO$_2$@Au/p53^{15} *d*-Ab and ATLP/SiO$_2$@Au/p53^{392} *d*-Ab. As shown in Fig. 2B, SiO_2@Au nanoparticles shows an apparent absorption peak at 520 nm (curve a), which corresponded to the typical resonance band of Au decorated on the surface of SiO_2. The peak of p53^{15} *d*-Ab and p53^{392} *d*-Ab posited at 280 nm (curves b and c), while the signal reporters ATCP and ATLP did not show any absorption peak (curves d and e). When the signal reporters (ATCP, ATLP) and detection antibody (*d*-Ab) were co-incubated with SiO_2@Au nanocarriers, the formed bio-conjugates presented two apparent absorption peaks at 280 nm and 520 nm (curves f and g), which indicated that the signal reporters and *d*-Ab have been successfully conjugated to the SiO_2@Au nanocomposites. Furthermore, the SWV responses demonstrated that pure p53^{15} *d*-Ab and SiO_2@Au nanoparticles did not show any signal (curves a, b in Fig. 2C), while the bio-conjugates of ATCP/SiO$_2$@Au/p53^{15} *d*-Ab displayed obvious responses at −0.808 V (curve c). The same SWV behaviors among p53^{392} *d*-Ab, SiO_2@Au and the ATLP/SiO$_2$@Au/p53^{392} *d*-Ab conjugates have also been tested (the data was not shown), which further proved that the signal reporters (ATCP and ATLP) have been successfully

loaded on the SiO_2@Au nanocarrier.

Moreover, the ratio of signal reporters and detection antibody (*d*-Ab) (ATMP/*d*-Ab) co-immobilized on SiO_2@Au nanocarriers is another key parameter to affect detection sensitivity. As shown in Fig. 2D, the current response increased with the increasing ratio of ATMP/*d*-Ab and then decreased at 210/1, indicating that the increase of signal reporter might decrease the immuno-coupling efficiency of *d*-Ab. Thus, the ratio of 210/1 (ATMP/*d*-Ab) was selected for preparation of ATCP/SiO_2@Au/p53^{15} *d*-Ab, ATLP/SiO_2@Au/p53^{392} *d*-Ab bio-conjugates. (ATMP: Apoferritin templated metallic phosphate)

3.3. Evaluation of immunoaffinities and optimization of incubation time among MP-c-Ab, phospho-proteins and d-Ab conjugate

As an accurate and quality-sensitive analytical measurement, EQCM has been successfully used to characterize the immunorecognition between nanomaterial-functionalized antibody and antigen (Ge et al., 2013). Herein, the affinity among MP-p53^{15} *c*-Ab, phospho-p53^{15} and ATCP/SiO_2@Au/p53^{15} *d*-Ab or MP-p53^{392} *c*-Ab, phospho-p53^{392} and ATLP/SiO_2@Au/p53^{392} *d*-Ab was monitored in real time by observing the frequency decreases (Δf), as shown in Fig. 3A. The QCM of the chip pre-incorporated with MP-p53^{15} *c*-Ab or MP-p53^{392} *c*-Ab was balanced firstly in Tris–HCl solution until a smooth and stable baseline was presented and lasted for another 40 min. After adding sample solution of phospho-p53^{15} or phospho-p53^{392}, a decreased response of Δf appeared due to the immunoreaction of MP-*c*-Ab and phospho-proteins. When ATCP/SiO_2@Au/p53^{15} *d*-Ab or ATLP/SiO_2@Au/p53^{392} *d*-Ab was introduced, an obvious decrease of Δf was obtained as expected, caused by the specific immunoaffinity to apoferritin *d*-Ab conjugates. At the same time, we could observe that the sandwich immuno-reactions of phospho-p53^{15} and phospho-p53^{392} were completed within 55 min and 65 min, respectively. The incubation time among MP-*c*-Ab, phospho-p53 and *d*-Ab conjugates was also optimized by electrochemical response, as showed in Fig. 3B. In the two immunoreactions (MP-c-Ab and phospho-p53, phospho-p53 and *d*-Ab conjugates), the current responses increased with the increasing incubation time, and reached a stable level after about 60 min, which was consistent with the QCM results.

3.4. Electrochemical simultaneous detection of phospho-p53^{15} and phospho-p53^{392}

Under optimized experimental conditions, the proposed multiplex immunosensor was conducted with different concentrations of sample solution containing both phospho-p53^{15} and phospho-p53^{392}. As shown in Fig. 4, the SWV response increased with the increasing concentration of phospho-p53^{392} and phospho-p53^{15} at -0.547 V and -0.808 V (Fig. 4A). The obtained current responses showed better linear relations over 0.1–20 ng/mL of phospho-p53^{15} and 0.05–20 ng/mL of phospho-p53^{392}, (Fig. 4B) than that of ELISA kit: 0.312–20 ng/mL of phospho-p53^{15} and 0.045–3 ng/mL phospho-p53^{392} (**Catalog #DYC1839-2, DYC2996-2 in R&D company**). The detection limit was 0.05 ng/mL and 0.02 ng/mL for phospho-p53^{15} and phospho-p53^{392}, respectively. The high sensitivity for simultaneous detection of multiple proteins was achieved by different apoferritin templated metallic phosphates as distinguishable signal reporters in the proposed immunoassay.

To further investigate the selectivity of the method, the immunosensor was incubated in human serum samples spiked with 1.0 ng/mL phospho-p53^{15}, phospho-p53^{392} and different possible interfering agents such as p53, phospho-p53^{46}, BSA and IgG. No remarkable electrochemical response change was observed for the mixed sample in comparison to the result obtained only in the presence of phospho-p53^{15}, phospho-p53^{392}, indicating good selectivity of the immunosensor.

A series of phospho-p53^{15} and phospho-p53^{392} spiked human serum samples pre-treated by filtration and dilution was used to validate the immunosensor. As summarized in Table 1, the recoveries are in the range of 93.5–106.6%, indicating that the immunosensor is reliable. In addition, the immunosensor could be stored at 4 °C. In this way, over 90% of the initial response remained after 1 week and 80% of the initial response remained after 1 month, indicating acceptable stability.

We evaluated the reproducibility of the immunosensor by simultaneous detection of the two target analytes for five groups. The obtained results showed the variation coefficients of 6.3% for 2.0 ng/mL p53^{15} and 5.0ng/mL p53^{392}, respectively, which proved the acceptable reproducibility of the developed immunosensor.

4. Conclusion

In summary, a highly sensitive electrochemical immunosensor for simultaneous detection of multiplex analytes (phospho-p53^{15} and phospho-p53^{392}) was developed. Apoferritin with the hollow structure played the role of microreactor to form different metallic phosphates inside the cavity as voltammetrically distinguishable signal reporters to greatly enhance detection signal. Due to the distinguishable peaks in voltammogram for Pb^{2+} and Cd^{2+}, simultaneous detection of phospho-p53^{15} and phospho-p53^{392}) was archived. Additionally, SiO_2@Au nanocomposites were used as carriers to co-immobilize signal reporters and detection antibody, further improving detection sensitivity. The use of magnetic MP-*c*-Ab in the immunosensor developed in this work avoided multiple washing steps which are necessary in a traditional immunoassay. The developed electrochemical immunosensor showed excellent performance for simultaneous detection of phospho-p53^{15} and phospho-p53^{392}. The proposed method which uses different apoferritin templated metallic phosphates as distinguishable signal reporters showed great potential for simultaneous detection of multiple protein biomarkers.

Acknowledgment

This work was supported by the National Natural Science Foundation of China (21575047, 21275062) and the Centers for Disease Control and Prevention/National Institute for Occupational Safety and Health (CDC/NIOSH) Grant no. R21OH010768. Its contents are solely the responsibility of the authors and do not necessary represent the official views of CDC. XG would like to acknowledge the fellowship from the China Scholarship Council (CSC).

References

Appella, E., Anderson, C.W., 2001. Eur. J. Biochem. 268, 2764–2772.
Ashcroft, M., Kubbutat, M., Vousden, K., 1999. Mol. Cell. Biol. 19, 1751–1758.
Bar, J.K., Slomska, I., Rabczyński, J., Noga, L., Grybos, M., 2009. Int. J Gynecol. Cancer 19, 1322–1328.
Bernal, F., Tyler, A., Korsmeyer, S., Walensky, L., Verdine, G., 2007. J. Am. Chem. Soc. 129, 2456–2457.
Bode, A.M., Dong, Z., 2004. Nat. Rev. Cancer. 4, 793–805.
Chen, A., Bao, Y., Ge, X., Shin, Y., Du, D., Lin, Y., 2012. RSC Adv. 2, 11029–11034.
Douglas, T., Dickson, D.P.E., Betteridg, S., Charnock, J., Garner, C.D., Mann, S., 1995. Science 269, 54–57.
Du, D., Wang, J., Dohnalkova, A., Lin, Y., 2011a. Anal. Chem. 83, 6580–6585.
Du, D., Chen, A., Xie, Y., Zhang, A., Lin, Y., 2011b. Biosens. Bioelectron 26, 3857–3863.
Du, D., Wang, L.M., Shao, Y.Y., Wang, J., Engelhard, M.H., Lin, Y., 2011c. Anal. Chem. 83, 746–752.
Du, D., Zou, Z.X., Shin, Y., Wang, J., Wu, H., Engelhard, M.H., Liu, J., Aksay, I.A., Lin, Y.,

2010. Anal. Chem. 82, 2989–2995.
Evan, G.L., Vousden, K.H., 2001. Nature 411, 342–348.
Ge, X., Zhang, W., Lin, Y., Du, D., 2013. Biosens. Bioelectron. 50, 486–491.
Ge, X., Asiri, A.M., Du, D., Wen, W., Wang, S., Lin, Y., 2014. TrAC Trends Anal. Chem. 58, 31–39.
Iwahori, K., Yoshizawa, K., Muraoka, M., Yamashita, I., 2005. Inorg. Chem. 44, 6393–6400.
Jiang, T., Song, Y., Wei, T., Li, H., Du, D., Zhu, M., Lin, Y., 2016. Biosens. Bioelectron. 77, 687–694.
Kazuyasu, S., Julio, E.H., Shin'ichi, S., Toru, M., Michael, B., Alex, V., Carl, W.A., Ettore, A., 2013. Genes Dev. 12, 2831–2841.
Lai, G., Yan, F., Wu, J., Leng, C., Ju, H., 2011. Anal. Chem. 83, 2726–2732.
Lin, Y., Wang, J., Liu, G., Wu, H., Wai, C., Lin, Y., 2008. Biosens. Bioelectron. 23, 1659–1665.
Liu, G., Wang, J., Wu, H., Lin, Y., 2006. Anal. Chem. 78, 7417–7423.
Liu, G., Wu, H., Dohnalkova, A., Lin, Y., 2007. Anal. Chem. 79, 5614–5619.
Liu, G.D., Lin, Y.H., 2007. J. Am. Chem. Soc. 129, 10394–10401.
Minamoto, T., Buschmann, T., Habelhah, H., Matusevich, E., Tahara, H., Boerresen-Dale, A.L., Harris, C., Sidransky, D., Ronai, Z., 2001. Oncogene 20, 3341–3347.
Okuda, M., Iwahori, K., Yamashita, I., Yamashita, I., 2003. Biotechnol. Bioeng. 84, 187–194.
Polanams, J., Ray, A.D., Watt, R.K., 2005. Inorg. Chem. 44, 3203–3209.
Ptacek, J., Devgan, G., Michaud, G., Zhu, H., Zhu, X., Fasolo, J., Guo, H., Jona, G., Breitkreutz, A., Sopko, R., McCartney, R.,R., Schmidt, M.,C., Rachidi, N., Lee, Soo-Jung, Mah, A.,S., Meng, L., Stark, M., Stern, D.,F., Virgilio, C.,D., Tyers, M., Andrews, B., Gerstein, M., Schweitzer, B., Predki, P.,F., Snyder, M., 2005. Nature 438, 679–684.
Shin, Y., Dohnalkova, A., Lin, Y., 2010. J. Phys. Chem. C 114, 5985–5989.
Song, Y., Luo, Y., Zhu, C., Li, H., Du, D., Lin, Y., 2016. Biosens. Bioelectron. 76, 195–212.
Tang, D.P., Yuan, R., Chai, Y.Q., 2008. Anal. Chem. 80, 1582–1588.
Tang, J., Tang, D.P., Niessner, R., Chen, G.N., Knopp, D., 2011. Anal. Chem. 83, 5407–5414.
Toledo, F., Wahl, G.M., 2006. Nat. Rev. Cancer 6, 909–923.
Uchida, M., Klem, M.T., Allen, M., Suci, P., Flenniken, M., Gillitzer, E., Varpness, L., Liepold, L.O., Yong, M., Douglas, T., 2007. Adv. Mater. 19, 1025–1042.
Vousden, K.H., Lane, D.P., 2007. Nat. Rev. Mol. Cell. Biol. 8, 275–283.
Wang, H., Wang, J., Timchalk, C., Lin, Y., 2008. Anal. Chem. 80, 8477–8484.
Wang, J., Liu, G., Wu, H., Lin, Y., 2008. Small 4, 82–86.
Wilson, M.S., Nie, W.Y., 2006. Anal. Chem. 78, 2507–2513.
Wong, K.K.W., Mann, S., 1996. Adv. Mater. 8, 928–932.
Wu, Y., Chen, C., Liu, S., 2009. Anal. Chem. 81, 1600–1607.
Yang, Y., Asiri, A.,M., Tang, Z., Du, D., Lin, Y., 2013. Mater. Today 16, 365–373.
Yang, Y.Q., Tu, H.Y., Zhang, A.D., Du, D., Lin, Y.H., 2012. J. Mater. Chem. 22, 4977–4981.
Yap, D.B.S., Hsieh, J.K., Zhong, S., Heath, V., Gusterson, B., Crook, T., Lu, X., 2004. Cancer Res. 64, 4749–4754.
Yu, X., Munge, B., Patel, V., Jeensen, G., Bhirde, A., Gong, J.D., Kin, S.N., Gillespie, J., Gutkind, J., Papadimitrakopoulos, F., Rusling, J., 2006. J. Am. Chem. Soc. 128, 11199–11205.
Yuan, Y., Hua, X., Wu, Y., Pan, X., Liu, S., 2011. Anal. Chem. 83, 6800–6809.
Zhang, W., Asiri, A.M., Liu, D., Du, D., Lin, Y., 2014. TrAC Trends Anal. Chem. 54, 1–10.
Zhao, Y.T., Du, D., Lin, Y., 2015. Biosens. Bioelectron. 72, 348–354.
Zhu, C., Du, D., Eychmüller, A., Lin, Y., 2015. Chem. Rev. 115, 8894–8943.
Zhu, C., Yang, G., Li, H., Du, D., Lin, Y., 2015. Anal. Chem. 87, 230–249.